EPJ Web of Conferences **140**, 01002 (2017) DOI: 10.1051/epjconf/201714001002
Powders & Grains 2017

Clogging and unclogging of many-particle systems passing through a bottleneck

Iker Zuriguel[1,⋆], *Álvaro* Janda[2], *Roberto* Arévalo[3], *Diego* Maza[1], and *Ángel* Garcimartín[1]

[1] *Departamento de Física, Facultad de Ciencias, Universidad de Navarra, E-31080 Pamplona, Spain*
[2] *Particle Analytics Ltd, Alrick Building, Max Born Crescent, The King's Buildings, Edinburgh, EH9 3BF, UK*
[3] *Division of Physics and Applied Physics, School of Physical and Mathematical Sciences, Nanyang Technological University, 25 Nanyang Link, 637371, Singapore*

Abstract. When a group of discrete particles pass through a narrowing, the flow may become arrested due to the development of structures that span over the size of the aperture. Then, it is said that the system is clogged. Here, we will discuss about the existence of a phase diagram for the clogged state that has been recently proposed, arguing on its usefulness to describe different systems of discrete bodies ranging from granular materials, to colloidal suspensions and live beings. This diagram is built based on the value of a flowing parameter which characterizes the intermittent flow observed in all these discrete systems provided that there is an external or internal energy supply. Such requirement, which is necessary to destabilize the clogging arches, is absent in a standard static silo, which is therefore examined as a particular case. This view will help to understand some *a priori* inconsistencies concerning the role of driving force in the clogging process that have been found in the last years.

Consider a container full of grains with an orifice at the bottom which is continuously shaken up and down. If the relative size of the outlet with respect to the particles is not too large, an arch can be spontaneously developed arresting the flow. If the shaking intensity is strong enough, this clog could be eventually destroyed resuming the flow [1]. As a result, we have an intermittent flow of grains where avalanches of grains alternate with lapses of time during which the orifice is blocked. In a series of papers, it has been reported that the avalanche duration distribution decays exponentially suggesting a Poisson process governed by a constant probability of clogging over the whole duration of the avalanche [2, 3]. On the other hand, the lapses of time during which the orifice is blocked have been proved to display a power-law decay [3, 4] indicating a temporal dependence of the probability that the arches become destabilized. The origin of the power-law decay for the unclogging process is still not fully understood [5] although it could be related with creeping motion [6] due to friction.

1 Flowing parameter

Considering the different distributions observed for the clogging and the unclogging processes, the intermittent flow of grains through apertures (Fig. 1) can be characterized by the the flowing parameter Φ which is nothing but the average fraction of time that the grains are flowing:

$$\Phi = \frac{\langle t_f \rangle}{\langle t_c \rangle + \langle t_f \rangle} \tag{1}$$

where $\langle t_f \rangle$ is the average duration of the avalanches and $\langle t_c \rangle$ the average duration of clogs [4]. Note that $\langle t_f \rangle$ is always well defined as it corresponds to the first moment of an exponential distribution. Oppositely, $\langle t_c \rangle$ may not be defined: as stated above the clogging duration distribution always exhibits a power law decay $t_c^{-\alpha}$, the first moment of which only converges if $\alpha > 2$.

Having this in mind we can distinguish among three different scenarios. When the flow is continuous, and the silo never clogs, the flowing time is equal to the total measuring time, hence $\Phi = 1$ (Fig. 1a). When intermittencies appear $\Phi < 1$ and in this case, we can distinguish two situations. If the distribution of clogging times has an exponent $\alpha > 2$, then the average clogging time $\langle t_c \rangle$ is well defined and $0 < \Phi < 1$ (Fig. 1b). Otherwise, when $\alpha \leq 2$, the average of this distribution is not defined. In practical terms the measured $\langle t_c \rangle$ will increase with the temporal window in which the measurements are performed. In an hypothetical infinitely long measurement, one would obtain $\Phi = 0$ (sketched in Fig. 1c). At this point it should be stressed that differentiating among the scenarios represented in Fig. 1b and Fig. 1c is not straightforward unless the distribution of clogging times is obtained with sufficient statistical significance. To this end, the method introduced by Clauset et al. [7] has been employed in all the cases reported here. The flowing parameter Φ has an additional advantage from a practical point of view: if we

⋆e-mail: iker@unav.es

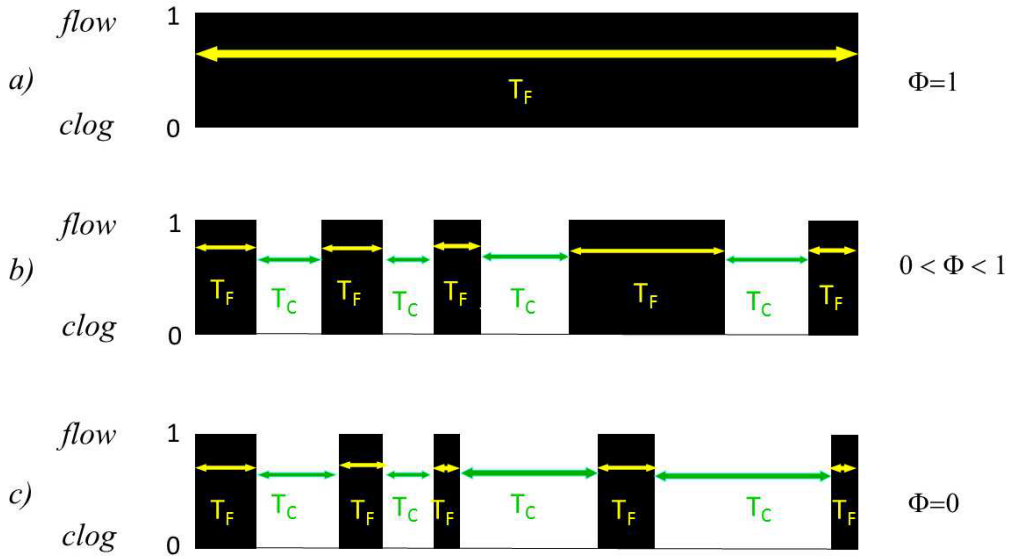

Figure 1. Scheme of the different flow situations that can be observed in the discharge of a vibrated silo. At each time the system is either flowing (*signal* = 1) or arrested (*signal* = 0). On the right, the value of the flowing parameter Φ that characterizes the type of flow. Φ = 1, continuous flow; 0 < Φ < 1, intermittent unclogged flow; and Φ = 0, clogged system. Note that, as explained in the text, the differences among the two last scenarios cannot be recognized unless a statistical analysis of the clogging time distribution is performed.

consider the flow rate during the flowing interval (W_i) we can straightforwardly obtain the average flow rate (considering intermittencies) as $W = \Phi W_i$. This is so because the flow rate during the flowing interval seems to be practically independent on the vibration amplitude (assuming that this is not too large) [2]. In addition, this W_i corresponds to the flow rate it will be obtained in an static silo, a topic that has been largely studied from Beverloo [8] until very recently (see [9] and references therein).

In Fig. 2 we show results of the flowing parameter versus the outlet size for a hopper vibrated continuously at the base and discharged eccentrically as explained in [3]. Different symbols are used for different vibration intensities Γ. The excitation can be approximated to a sinusoidal oscillation which intensity is:

$$\Gamma = \frac{A4\pi^2 f^2}{g} \tag{2}$$

where A is the amplitude, f the frequency, and g the gravity acceleration. In our works, we typically set a constant frequency and change A. In Fig. 2 the flowing parameter was calculated by measuring the average of both, the flowing and the arrest intervals. In all the cases, special attention was paid to the distribution of clogging times. For the case of $\alpha \leq 2$ the value for Φ was set to zero even though, in the finite temporal window in which the measurement was performed, some flowing intervals were observed, as in Fig 1c.

2 Unclogging diagram

From the results displayed in Fig. 2 it becomes evident that for all the intensities of vibration studied, a transition from Φ = 0 to Φ > 0 occurs for a given outlet size. As it could be anticipated, the smaller Γ is, the larger the outlet at which the transition takes place. From these data, we can sketch a 2D phase diagram such as in Fig. 3 where we use stars to represent points where Φ = 0 and open circles for Φ > 0. The dashed curve suggests the possible transition between two phases: a clogged one when Φ = 0, and an unclogged one when Φ > 0. Note that the latter can be intermittent or continuous depending on wether Φ < 1 or Φ = 1. The study of such intermittent to continuous flow transition is not the aim of this manuscript; instead we will focus in the transition from unclogged to clogged based on the properties of the intermittent flow.

Indeed, the same features of the intermittent flow described above have been observed in other bidimensional silos, and also in disparate systems such as colloids flowing through an orifice, sheep passing through a narrow gate and pedestrians evacuating a room through a narrow door. In all cases, the distribution of flowing times is exponential and the one of the clogging times displays a power law decay. Of course, depending on the system, the variables affecting the value of the exponent α are different (table 1).

In a 2D flat bottomed silo vibrated as a whole we found that the transition from clogged to unclogged state can be achieved by increasing the outlet size and increasing the external vibration [4]. This confirmed the results presented above for the 3D case and enlarged the scope of this phenomenon, which seems to occur independently of the dimensionality of the problem, the geometry of the outlet (symmetric orifice in a flat bottom or asymmetric hopper) and the nature of the vibration (local or global). In ad-

dition, in this 2D flat bottomed silo we observed that the transition from clogged to unclogged can be also attained by reducing the amount of grains above the orifice. This suggests that the weight of the material above the arch prevents the clog destruction (for a given vibration intensity and outlet size). To confirm this idea, we performed independent experiments in a tilted 2D hopper which inclination (measured by the angle that the silo plane makes with the gravity direction) could be varied at will. Interestingly, for a given value of shaking intensity and outlet size, the system was clogged when the silo was vertical and the transition to unclogged appeared when the inclination became more horizontal. This confirms that arches with smaller load above them are broken easier than the ones with more load.

As stated above, another system in which the intermittent flow was observed was a suspension of colloidal particles passing through a small orifice. Simulations were performed with the lattice-Boltzmann method, incorporating 128 discrete solid spherical particles (more information about the numerical method can be found in [4]). The fluid was submitted to a uniform force perpendicular to a wall with a circular orifice at the center, mimicking a pressure driven flow that pushes the colloidal particles through an opening. As a consequence, an accumulation of the colloidal particles was observed in the neighbourhood of the orifice which eventually caused the formation of a clog. Long time simulations were required to obtain sufficient statistics of the clogging events. To this end, in each simulation the colloidal particles were allowed to cross several times the system size, being reinjected at the backwards of the system each time they crossed the outlet. For each simulation conditions, the passage time of around 10^5 colloidal particles was registered. Two different scenarios were simulated with different temperatures (which controls the interplay between colloidal particle fluctuations and the intensity of the driving force). The flow was observed to be intermittent, displaying (as in the case of silos) power law decays for the clogging times and exponential distributions for the flowing intervals. As expected, low temperatures lead to clogged states ($\phi = 0, \alpha \leq 2$), and high temperatures to unclogged states ($\phi > 0, \alpha > 2$).

With the idea of further extending this description to other systems, we performed experiments of sheep entering a barn through narrow gates. Details of these tests can be found in [4, 10–12] but they basically consisted on registering the entrance (one per day) of 100 sheep to a barn where food is placed. The recording was performed with two videocameras (one inside the barn and the other outside). From the movies, spatiotemporal diagrams were made in which the passage time of each sheep was measured. Again, the intermittent flow was studied evidencing power law decays for the clogging times and exponential distributions for the flowing intervals. For safety reasons, we never observed a transition to a clogged phase, but several parameters were shown to affect the exponent of the power law. The first one was the gate size: the smaller the gate, the lower the exponent, hence suggesting that for a sufficiently small door, it would be possible to reach $\alpha \leq 2$.

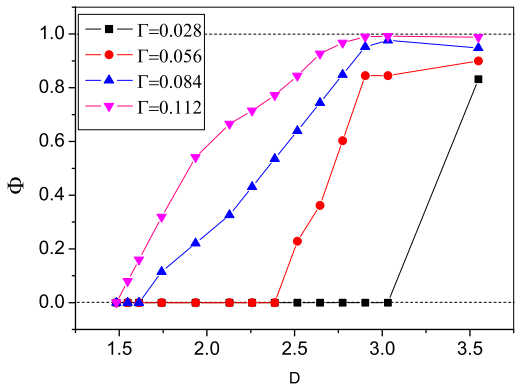

Figure 2. Flowing parameter Φ versus the rescaled outlet size D for different values of vibration intensity Γ in a locally vibrated eccentrically discharged hopper as the one described in [3].

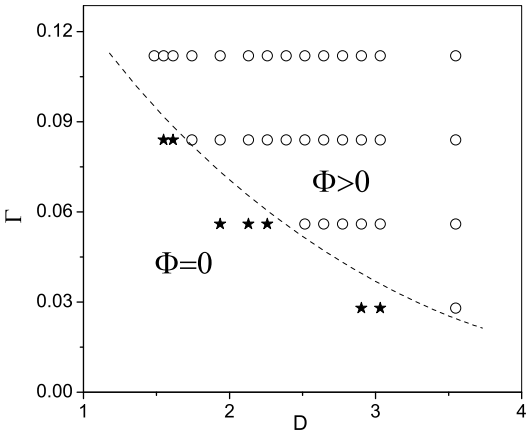

Figure 3. Phase diagram for the plane $\Gamma - D$ obtained for a locally vibrated eccentrically discharged hopper [3]. Stars indicate points where $\Phi = 0$ (clogged phase) and circles show positions where $\Phi > 0$ (unclogged phase). The dashed line is a guide to the eye suggesting a possible boundary between the two phases.

Another one was the presence of an obstacle in front of the door. Interestingly, if the obstacle is placed at an appropriate position the exponent increases and the flow improves (there are fewer clogs and they last less time). Of course, if the obstacle is too far from the door, its effect is negligible and if it is too close it could be even detrimental as clogs appear between the obstacle and the door (instead of at the very door) [11]. The effect of the obstacle in the flow rate through narrow doors has been traditionally attributed to the waiting-room effect: the obstacle controls the inflow of animals preventing overcrowding the constriction region. Interestingly, we show that it also has an effect on facilitating resuming the flow, surely due to a pressure reduction at the door which may also be linked to an increase of sheep mobility that can lead to a raising of sheep "temperature". The final variable that was shown to affect the exponent is the competitiveness of the sheep [12].

Table 1. Parameters that have been observed to affect the exponent α of the power law decay of clogging times in the different systems studied. Arrows indicate the direction in which the variables have to be modified in order to increase α and improve the flow. The variables marked in bold are the ones in which the transition from clogged ($\alpha \leq 2$, $\phi = 0$) to unclogged ($\alpha > 2$, $\phi > 0$) has been observed. In the other ones, we expect such transition but it cannot be attained experimentally for safety reasons. All the variables in each column have been grouped with a single name following the spirit of [15]. Italics are used to denote that the obstacle effect is not definitively proved to be linked with a reduction of compatible load or an increase of the temperature.

	Typical length (Λ)	Incompatible Load (I_L)	Compatible Load (C_L)
2D granular silo	↑ **outlet size**	↑ **external global vibration**	↓ **height of the layer of grains**
2D granular hopper			↓ **inclination**
3D granular eccentric hopper	↑ **outlet size**	↑ **external local vibration**	
colloids		↑ **temperature**	
sheep	↑ gate size	*placing an obstacle*	*placing an obstacle* & ↓ motivation
pedestrians (simulations)	↑ **gate size**	↑ **internal noise**	↓ **motivation**
pedestrians (experiments)	↑ gate size		↓ motivation

Indeed, tests performed during warm conditions (summer time at 3 pm Spanish time) lead to a reduction of clogging events compared with standard measurements carried out in cooler circumstances (in the morning during the rest of the year). This was attributed to a noticeable reduction of the eagerness of sheep in warmer days which implies that the higher the competitiveness of the animals the less efficient is the entrance. Indeed, this behavior was already predicted for human evacuation through narrow doors by Helbing et al. [13] and was given the name of "Faster is Slower" suggesting that the faster the pedestrians aim to escape, the slower is the process.

In other series of experiments performed in the University of Navarra, this "Faster is Slower" effect was proved experimentally with real people [12]. A group of around 80-90 volunteers were instructed to evacuate a room with different competitiveness. This was quantified by measuring the velocity of the people at the beginning of the evacuation (before the density in front of the door built up and clogs started to appear) and a good correlation was observed: the higher the competitiveness, the higher the initial velocity. In addition, pioneer pressure measurements were performed at the doorjamb, also showing an increase of the registered values as the competitiveness grew higher. As in previous cases, intermittencies in the flow rate were analysed and the outcomes evidenced an exponential tail of bursts sizes and a power law decay for the clogging times. Moreover, pedestrian evacuations also evidenced that the larger the door size the higher the exponent of the power law tail [14] as it happens for sheep and granular media.

Finally, numerical simulations of pedestrian evacuations were used to confirm that both, reducing competitiveness and enlarging the door size, improve the flowability (as they lead to an increase of the exponent of the power law decay). In addition, these simulations revealed that increasing the internal noise of the simulated bodies did also produce an increase of the exponent of the power law decay. Contrary to the experiments, these simulations could be extended to situations where clogs were much more stable, and the transition to $\alpha \leq 2$ ($\phi = 0$) attained.

All the findings concerning the ways in which different variables affect the exponent value in such disparate systems are summarized in table 1. The arrows indicate the direction in which the variables should be tuned to increase α and bold letters are used to stress the cases where the transition from clogged to unclogged has been obtained. Considering these outcomes, we have grouped the different specific variables in three general groups. In the first column of table 1, we place those variables that are related to the size of the orifice (or the relation between the size of the orifice and the size of the particles). In the second column we find parameters that are related to the excitation that particles intrinsically have or at which they are submitted. This is a kind of temperature or, more generally speaking, an *Incompatible Load* (I_L) in the sense that it is a stress made in a direction which is different from that of the force that caused the blockage. Finally, in the third column we have grouped variables related to a *Compatible Load* (C_L) indicating that there are forces acting in the same direction that the one driving the system towards the clogged situation. Note that the terminology of Compatible Load and Incompatible Load has been taken from [15] which was indeed the work that inspired A. Liu and S. R. Nagel to propose the groundbreaking idea of the jamming phase diagram in [16].

Considering the grouped variables in table 1 and the shape of the phase diagram obtained for the plane $\Gamma - D$ in Fig. 3, we can speculate about the existence of a clogging phase diagram as the one sketched in Fig. 4. The variables at play will be the ones mentioned above: a lengthscale, Λ; the Incompatible Load, I_L; and the Compatible Load, C_L. Increasing Λ and I_L, and reducing I_L leads to a transition from the clogged to the unclogged phase. Therefore, in analogy with the packing fraction in the jamming diagram [16], the compatible load is written as $1/C_L$ in the clogging phase diagram. It is important to remark that this clogging phase diagram is just a concept which is proposed based on the findings obtained in many different systems. Now, it becomes necessary to characterize quantitatively each of the diagram planes with the aim of assessing the kind of transition that clogging is. It would not be surprising that the specific nature of the transitions depend on the system. However, the unified proposed scenario allows to point out some generic issues that are, in our opinion, relevant. The presence of a characteristic length scale

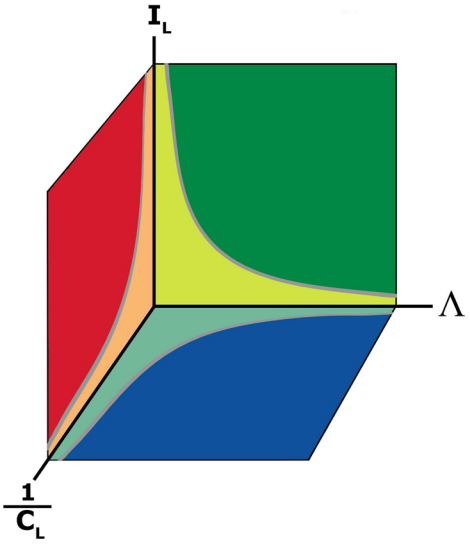

Figure 4. Clogging phase diagram proposed in [4]. Within the light surface the system would be in a clogged phase and outside it, in an unclogged phase. The generic variables are the Length Scale, Λ; the Incompatible Load, I_L; and the Compatible Load, C_L.

stresses the finite-size nature of clogging, where the outlet size competes with the scale of the structures formed near the outlet. Surely, such a scale will strongly depend on the specific properties of the many-body system we are dealing with: cohesive or faceted grains [18–22], for example, will imply a larger characteristic size. The insight gained in this work also allows us to explain the increased stability of clogs exhibited by suspensions when are subjected to higher fluid velocities [17] or helps to understand the origin of Faster is Slower effect found in pedestrian dynamics.

3 The static silo as a special case

Up to now, we have described the intermittent flow in a vibrated silo and defined a phase transition depending on whether the first moment of the distribution of clogging times converges or not. Then, we have extended the analysis of this property of the intermittent flow to other different systems leading to the proposal of a generic clogging phase diagram. Now, we can go back to the case of the silo and study what it seems to be the simplest case of a standard non-vibrated one. The first issue that becomes evident is that, once there is an arch that blocks the outlet, the flow becomes forever arrested. In practical terms, this constitutes a drawback as the distribution of clogging times is not accessible any more: all clogs last an infinite time. Therefore, it could naively thought that the problem is simpler and, in order to decide if we are in a clogged phase or not, it suffices to build a silo with an orifice at the bottom and see if, eventually, there is an arch that arrests the flow. Paradoxically, the situation is much more complex than expected and, despite the numerous efforts devoted to unveil if there is a transition from clogged to unclogged regimes, there is not a robust and definitive answer yet.

At this time, it has been shown that both the avalanche duration and the avalanche size distributions display an exponential tail analogous to the flowing times interval distribution observed in the vibrated silo [23–35]. This exponential tail, which extends to other systems such as fluid driven particle flow [36, 37] has been explained in terms of the existence of a constant probability of clogging [28, 38, 39]. Only for the case of very elongated orifices (slits) a power law decay was observed which was justified as a convolution of many exponential distributions with different exponents [40].

Concerning the existence of a transition from a clogged to an unclogged phase, the most studied variable is the mean avalanche size $\langle s \rangle$ which has been shown to abruptly increase with the outlet size [24]. Remarkably, in a three-dimensional silo an augment of the outlet diameter from $D = 2$ to $D = 5$ (measured in number of particles' diameters) leads to an increase of the avalanche size in around 7 orders of magnitude. The first fitting proposed to explain this sudden growth was a critical power law that diverges at a given critical value D_C. This implies that, above this value, clogging events are not possible. Subsequently, it was proposed that other fittings were equally valid. In particular it was suggested that $\langle s \rangle$ could grow exponentially: e^{CD^2} in a two-dimensional system and e^{CD^3} in a three-dimensional one (where C is a constant) [30]. For the two-dimensional case there seems to be a consensus about the appropriateness of both fittings, and indeed there are models that justify only the nondivergent approach [31, 32]. Otherwise, the three-dimensional silo is still controversial as some results plea in favor of the nondivergent scenario [32] whereas others [31] evidence that the e^{CD^3} fitting is not valid.

Having this controversy in mind and the methodological difficulty we find to define the transition, we can still see how the static silo could fit into the generic framework presented in Fig. 4. Clearly, if such transition exists, it must be abrupt as the flowing parameter could only take values of $\Phi = 0$ (if there is clogging) or $\Phi = 1$ if there is not clogging. The intermittent unclogged regime ($0 < \Phi < 1$) does not exist as, once the silo clogs, nothing can resume the flow. This is so because the Incompatible Load (vibration) is 0 due to the absence of external vibration. At this point we would like to note that previous to the arrest of the flow, the energy of the particles within the silo can be considerably large. Therefore, if we want to strictly explore the plane $I_L = 0$, an experiment where the grains are extracted without velocity (in a quasistatic way) is necessary.

A possibility that has been explored in the recent years is to increase the driving force (i.e. the gravity) and see the effect on the clogging probability. This has been done by means of numerical simulations [33, 34] in a 2D non-vibrated silo. In both works, we used soft-particle molecular dynamics simulations of equally sized disks. The restoring force in the normal direction of collision depends linearly on the particles overlap $\xi = d - r_{ij}$, with stiffness

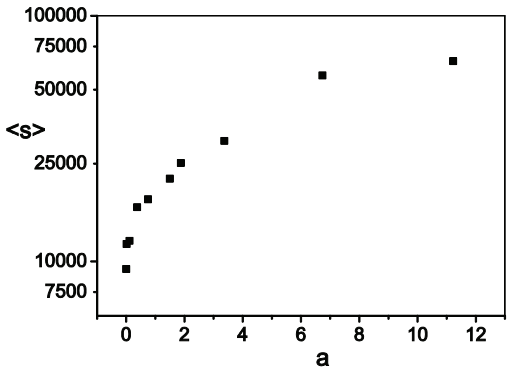

Figure 5. Average avalanche size (in logarithmic scale) versus the external field a measured in units of the gravity acceleration g. Numerical results, obtained with the model explained in [34] are displayed for for a 2D silo with $D = 5$.

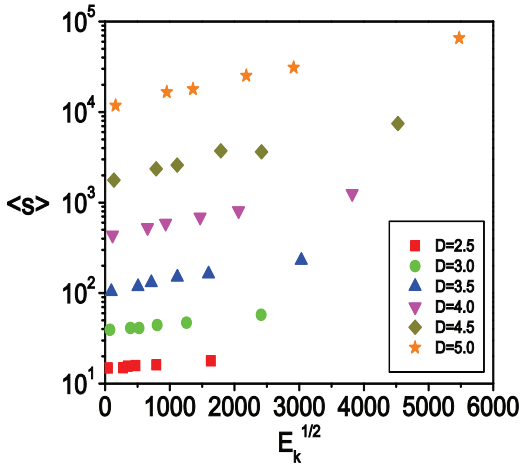

Figure 6. Numerical results of the average avalanche size (in logarithmic scale) versus the kinetic energy E_k within the whole system for different outlet sizes as indicated in the legend.

$k_n = 10^5(mg/d)$, where $d = 1\ mm$ is the particle diameter, $m = 1$ is the mass and r_{ij} the distance between the centers of the particles. Additionally, there is a dissipative force proportional to the relative normal velocity of the colliding grains, with damping parameter $\gamma_n = 300(m\sqrt{g/d})$. We implement static friction placing a spring in the direction tangential to the normal joining the centers of the particles. The elongation of this spring is obtained integrating the relative velocity of the surfaces in contact. The parameters are $k_t = (2/7)k_n$ and $\gamma_t = 200(m\sqrt{g/d})$. The friction coefficient is set to $\mu = 0.5$, and the gravity to a times the value of g. In order to optimize the computing time, we use a integration step $\delta = 10^{-4}\sqrt{d/g}$ for simulations with $a \simeq 1$. For $a \simeq 3$ the integration step is $\delta/3$, and for simulations at $a \simeq 6$ and $a \simeq 10$ we use a step of $\delta/6$. For simulations at $a \simeq 10^{-3}$ we increase the time step to 10δ to assure that collisions are simulated with sufficient accuracy. Importantly, note that in the different simulated scenarios the values of k_n, k_t, γ_n, and γ_t were constant (independent on the value of a). Also, it should be stressed that the selected value of k_n assures that in all the simulations the elastic deflections are very small compared to particle radii.

Despite that within this framework one may expect that results obtained with different driving forces might not depend on gravity (dimensionless results should only depend on dimensionless combinations of the input parameters) it is observed that increasing gravity leads to an increase of the mean avalanche size, i.e. a reduction of clogging probability [33, 34]. Indeed, this increase of the avalanche size with gravity depends on the outlet size (the larger the outlet the stronger the effect) and is not very pronounced: for the largest outlet size studied (Fig. 5) an increase of $\langle s \rangle$ in one order of magnitude is obtained by increasing the driving force a in four orders of magnitude (from $a = 10^{-3}$ to $a = 10$ times the gravity value). The origin of this increase was discarded to be caused by the fact that the higher the external field, the stronger the weight that the arches have to resist [33]. Instead, it was argued that the origin was related to the increase of the average kinetic energy of the flowing grains caused by the augment of the gravity which is, perhaps, not compensated by a corresponding augment of the dissipation (recall that both dissipative terms γ_n and γ_t were chosen to be constant). In this sense, it was proposed that two conditions must be fulfilled in order to observe the clogging phenomenon: 1) an arch should be formed at the orifice; 2) the arch should resist until all the kinetic energy in the system dissipates. Increasing the driving force leads to a linear increase of the kinetic energy of the grains that has to be dissipated and therefore to an increase of the probability that an arch gets destabilized before the whole system comes to a rest. Based on this idea, in Fig. 6 we represent the mean avalanche size (in logarithmic scale) versus the square root of the total kinetic energy of the grains within the silo. Clearly, for all the outlet sizes the higher the kinetic energy, the larger the avalanche size. In addition, it is observed that there seems to be a limit avalanche size when the kinetic energy vanishes (for very low driving forces). This limit avalanche sizes clearly depends on the outlet size. Nevertheless, the growth rate of the avalanche with the kinetic energy, seems to be rather independent on the outlet size, yet a small dependence has been observed: the higher the outlet size is, the faster is the growth rate.

From all these numerical outcomes, it was concluded that in a static silo the higher the driving force the larger the avalanche size. This somehow contradicts the behaviour expected from the clogging transition diagram proposed in Fig. 4. Indeed, it can be definitively stated that in a static silo, faster is faster, and also the faster the grains flow, the less likely that a clog develops. Having said that, it is also true that gravity does not play a crucial role in clogging development if it is compared to the effect that it has on the flow rate [41]. Indeed, the most important parameter determining clogging is the outlet size: increas-

ing the outlet size from 4.5 to 5 has a stronger effect in the avalanche size than increasing the driving force from $a = 10^{-3}$ to $a = 10$. In any case, the fact that the driving force effect is related to the kinetic energy of the grains suggests that care should be taken when looking at the results of $\langle s \rangle$ vs the outlet size in the traditional way. And this is so because when we modify the outlet size we are increasing the required size of the clogging structures, but we are also increasing the kinetic energy within the system which is related with the above-mentioned probability of destabilization of an arch.

4 Conclusions

In this manuscript we have explained the origin and features of a recently proposed clogging phase diagram. This phase diagram differentiates among clogged and unclogged phases based on a statistical property of the flow intermittencies: in some situations the mean time of the lapses during which the flow is arrested cannot be defined, as the first moment of the distribution does not converge. The origin of this non-convergence hinges on the distribution of these clogging times which has been shown to be compatible with a power law decay. Independently of whether it is or not a power law, the distribution of clogging times is undoubtedly not an exponential as it would be expected if the probability that the arch becomes destabilized were constant over time. Otherwise, the unclogging probability decreases with time suggesting some kind of aging of the blocking structure which is probably associated to the dynamics of the particles behind it. Let us note that in a recent paper where clogging was observed in more diluted situations, the unclogging time distributions were observed to decay exponentially [42]. This reflects that the unclogging process in such a dilute situation is different to the dense systems analysed here.

The clogging phase diagram is useful to understand several features of the flow through constrictions of many different systems, ranging from colloids to pedestrians. In such systems, the common ingredients that are necessary to observe the clogging transition seem to be: 1) a bottleneck small enough in order to allow the formation of a geometrical structure spanning over its size; 2) a force that drives the system towards the outlet which is also necessary to stabilize the clogging structures; and 3) an internal or external agitation that is able to break the clogging structure and resume the flow. Paradoxically, if the latter condition is not fulfilled the problem becomes more complex as the arches cannot be destroyed and the strategy followed to study the transition (which is basically focused in the unclogging process) is not useful anymore. Otherwise, in a static silo the only process that can be studied is the clogging one.

At this point let us stress the importance of separating both processes, clogging and unclogging, to fully understand the dynamics of the flow of particles through bottlenecks. Clogging seems to occur randomly, with a probability that does not depend on time, whereas unclogging reveals temporal dependence. Indeed, distinct variables may affect both processes in different ways. For example, increasing the orifice size always improves the flow, preventing clogging and facilitating unclogging. However, the effect of increasing the driving force in the flow is not unique: it is beneficial because it prevents the development of clogging (as in the static silo), but it is also prejudicial because it precludes unclogging as the formed arches are stronger.

This different effect of the driving force in the clogging and unclogging processes causes the Faster is Slower effect. For low driving forces, the flow rate augments with it as the velocity of the particles increases (and clogging decreases). But eventually, for a given driving force, the arches that form become so strong that the dynamics becomes controlled by the unclogging process. Therefore, increasing the driving force leads to a reduction of the flow rate. From this reasoning, it becomes obvious that in a static silo, Faster is Slower cannot be observed as this effect is linked to the unclogging process.

Acknowledgements

We thank Ignacio Pagonabarraga, Daniel Ricardo Parisi, Luis Ariel Pugnaloni, Raúl Cruz Hidalgo, Celia Lozano, and Eric Clément for helpful discussions and LuisFer Urrea for technical help. This work has been funded by Ministerio de Economìa y Competitividad (Spanish Government) through Project No. FIS2014-57325.

References

[1] C. Lozano, G. Lumay, I. Zuriguel, R. C. Hidalgo, and A. Garcimartín, Phys. Rev. Lett. **109**, 068001 (2012).
[2] C. Mankoc, A. Garcimartín, I. Zuriguel, D. Maza and L. A. Pugnaloni, Phys. Rev. E **80**, 011309 (2009).
[3] A. Janda, D. Maza, A. Garcimartín, E. Kolb, J. Lanuza and E. Clément, Europhys. Lett. **87**, 24002 (2009).
[4] I. Zuriguel, D. R. Parisi, R. C. Hidalgo, C. Lozano, A. Janda, P. A. Gago, J. P. Peralta, L. M. Ferrer, L. A. Pugnaloni, E. Clément, D. Maza, I. Pagonabarraga and A. Garcimartín, Scientific Reports **4**, 7324 (2014).
[5] A. Nicolas, S. Bouzat, M. Kuperman, Phys. Rev. E **94**, 022313 (2016).
[6] B. Blanc, J. -C. Géminard, L. A. Pugnaloni, Eur. Phys. J. E **37**, 112 (2014).
[7] A. Clauset, C. R. Shalizi, and M. E. Newman, SIAM review **51**, 661-703 (2009).
[8] W.A. Beverloo, H.A. Leninger and J.J. van de Velde, Chem. Eng. Sci. **15**, 260 (1961)
[9] S.M. Rubio-Largo, A. Janda, D. Maza, I. Zuriguel and R.C. Hidalgo, Phys. Rev. Lett. **114**, 238002 (2015)
[10] A. Garcimartín, J. M. Pastor, L. M. Ferrer, J. J. Ramos, C. Martín-Gómez, and I. Zuriguel, Phys. Rev. E **91**, 022808 (2015).
[11] I. Zuriguel, J. Olivares, J. M. Pastor, C. Martín-Gómez, L. M. Ferrer, J. J. Ramos and A. Garcimartín, Phys. Rev. E **94**, 032302 (2016).

[12] J. M. Pastor , A. Garcimartín, P. A. Gago, J. P. Peralta, C. Martín-Gómez, L. M. Ferrer, D. Maza, D. R. Parisi, L. A. Pugnaloni and I Zuriguel, Phys. Rev. E. **92**, 062817 (2015).

[13] D. Helbing, I. J. Farkas , and T. Vicsek. Nature **407**, 487 (2000).

[14] A. Garcimartín, D.R. Parisi, J.M. Pastor, C. Martín-Gómez, and I. Zuriguel, J. Stat. Mech. **2016**, 043402 (2016).

[15] M. E. Cates, J. P. Wittmer, J. P. Bouchaud, and P. Claudin, Phys. Rev. Lett. **81**, 1841 (1998).

[16] A. J. Liu, and S. R. Nagel, Nature **396**, 21-22 (1998).

[17] J. R. Valdes, and J. C. Santamarina, Can. Geotech. J. **45**, 177-184 (2008).

[18] T. Kanzaki, M. Acevedo, I. Zuriguel, I. Pagonabarraga, D. Maza, and R.C. Hidalgo. The European Physical Journal E **34**, 133 (2011).

[19] D. Höhner, S. Wirtz, and V. Scherer. Powder Technology **226**, 16-28 (2012).

[20] F. Alonso-Marroquín, Á. Ramírez-Gómez, C. González-Montellano, N. Balaam, D. A. H. Hanaor, E. A. Flores-Johnson, Y. Gan, S. Chen, and L. Shen. Granular Matter **15**, 811-826 (2013).

[21] J. Tang, and R. P. Behringer. Europhysics Letters **114**, 34002 (2016).

[22] T. Borzsonyi, E. Somfai, B. Szabó, S. Wegner, P. Mier, G. Rose and R. Stannarius. New J. Phys. **18**, 093017 (2016).

[23] K. To *et al.*, Phys. Rev. Lett. **86**, 71 (2001).

[24] I. Zuriguel, A. Garcimartín, D. Maza, L. A. Pugnaloni, and J. M. Pastor, Phys. Rev. E **71**, 051303 (2005).

[25] J. Tang and R.P. Behringer, Chaos **21** 041107 (2011).

[26] L. Kondic, Granular Matter **16**, 235 (2014).

[27] S. Tewari, M. Dichter, and B. Chakraborty, Soft Matter **9**, 5016 (2013).

[28] I. Zuriguel *et al.*, Phys. Rev. E **68**, 030301 (R) (2003).

[29] C. C. Thomas and D. J. Durian, Phys. Rev. E 87, 052201 (2013).

[30] K. To, Phys. Rev. E **71**, 060301 (R) (2005).

[31] A. Janda, I. Zuriguel, A. Garcimartín, L. A. Pugnaloni, and D. Maza, Europhys. Lett. **84**, 44002 (2008).

[32] C. C. Thomas, D. J. Durian, Phys. Rev. Lett. **114**, 178001 (2015).

[33] R. Arévalo, I. Zuriguel, D. Maza, and A. Garcimartín, Phys. Rev. E **89**, 042205 (2014).

[34] R. Arévalo, and I. Zuriguel. Soft Matter **12**, 123-130 (2016).

[35] S. Mondal, M. M. Sharma, *Role of flying buttresses in the jamming of granular matter through multiple rectangular outlets*, Granular Matter **16**, 125-132 (2014).

[36] A. Guariguata, M. A. Pascall, M. W. Gilmer, A. K. Sum., E. D. Sloan, C. A. Koh, D. T. Wu, *Jamming of particles in a two-dimensional fluid-driven flow*, Phys. Rev. E **86**, 061311 (2012).

[37] P. G. Lafond, M. W. Gilmer, C. A. Koh, E. D. Sloan, D. T. Wu, A. K. Sum., *Orifice jamming of fluid-driven granular flow*, Phys. Rev. E **87**, 042204 (2013).

[38] D. Helbing, A. Johansson, J. Mathiesen, M. H. Jensen, A. Hansen, *Analytical approach to continuous and intermittent bottleneck flows*, Phys. Rev. Lett. **97**, 168001 (2006).

[39] T. Masuda, K. Nishinari, A. Schadschneider, *Critical Bottleneck Size for Jamless Particle Flows in Two Dimensions*. Phys. Rev. Lett. 112, 138701 (2014).

[40] S. Saraf, S V Franklin *Power-law flow statistics in anisometric (wedge) hoppers*, Phys. Rev. E **83**, 030301(R) (2011).

[41] S. Dorbolo, L. Maquet, M. Brandenbourger, F. Ludewig, G. Lumay, H. Caps, N. Vandewalle, S. Rondia, M. Mélard, J. van Loon, A. Dowson, S. Vincent-Bonnieu, Granular Matter **15**, 263 (2013).

[42] I. G. Tejada, L. Sibille and B. Chareyre, EPL **115**, 54005 (2016).